Neoadjuvant chemotherapy modulates the immune microenvironment in metastases of tubo-ovarian high-grade serous carcinoma

Authors and Affiliations

Steffen Böhm[1,4], Anne Montfort[1], Oliver M.T. Pearce[1], Joanne Topping[1], Probir Chakravarty[2], Gemma L.A. Everitt[1], Andrew Clear[1], Jackie R. McDermott[1,3], Darren Ennis[1,6], Thomas Dowe[1], Amanda Fitzpatrick[4], Elly C. Brockbank[5], Alexandra C. Lawrence[5], Arjun Jeyarajah[5], Asma Z. Faruqi[3], Ian A. McNeish[1,6], Naveena Singh[3], Michelle Lockley[1,4], Frances R. Balkwill[1*]

[1] Barts Cancer Institute, Queen Mary University of London, Charterhouse Square, London EC1M 6BQ UK

[2] Bioinformatics Core, The Francis Crick Institute, 44 Lincoln's Inn Field, London WC2A 3LY, UK.

[3] Department of Pathology, Barts Health NHS Trust, Newark Street, London E1 2ES, UK

[4] Medical Oncology, Barts Health NHS Trust, West Smithfield, London EC1A 7BE, UK

[5] Gynaecological Oncology, Barts Health NHS Trust, Whitechapel Road, London E1 1BB, UK

[6] Wolfson Wohl Cancer Research Centre, Institute of Cancer Sciences, University of Glasgow, G61 1QH, UK.

Running Title: Neoadjuvant chemotherapy and tumor immunity in ovarian cancer

Financial support: This research was funded by Swiss Cancer League (BIL KLS-2883-02-2012); the European Research Council (ERC322566); Cancer Research UK (A16354); Barts and The London Charity (467/1307).

Corresponding author: Prof. Frances Balkwill, Barts Cancer Institute, Centre for Cancer and Inflammation, Queen Mary University of London, Charterhouse Square, London, EC1M 6BQ, UK.

Tel: + 44 207882 3851

Fax: + 44 207882 3585

Email: f.balkwill@qmul.ac.uk

Disclosures: IM is on advisory boards for Advisory Boards for Clovis Oncology and Verastem. There are no other disclosures from the authors.

Translational Relevance: This research using samples from ovarian cancer patients shows that three to four cycles of platinum-based chemotherapy alters the functional orientation, activation status and density of certain T cell subsets in a tumor microenvironment and reduces systemic levels of tumor promoting cytokines. The results suggest that the effects of immunotherapy might be enhanced if given after chemotherapy, potentially improving disease control in patients with advanced HGSC and other cancer types.

Abstract

Purpose

The purpose of this study was to assess the effect of neoadjuvant chemotherapy, NACT, on immune activation in stage IIIC/IV tubo-ovarian high-grade serous carcinoma (HGSC), and its relationship to treatment response.

Experimental Design

We obtained pre- and post-treatment omental biopsies and blood samples from a total of fifty-four patients undergoing platinum-based NACT and six patients undergoing primary debulking surgery. We measured T cell density and phenotype, immune activation and markers of cancer-related inflammation using immunohistochemistry, flow cytometry, electrochemiluminescence assays and RNA sequencing and related our findings to histopathological treatment response.

Results

There was evidence of T cell activation in omental biopsies after NACT: $CD4^+$ T cells showed enhanced $IFN\gamma$ production and anti-tumor Th1 gene signatures were increased. T cell activation was more pronounced with good response to NACT. The $CD8^+$ T cell and $CD45RO^+$ memory cell density in the tumor microenvironment was unchanged after NACT but biopsies showing a good therapeutic response had significantly fewer $FoxP3^+$ T regulatory cells. This finding was supported by a reduction in a T regulatory cell gene signature in post versus pre NACT samples that was more pronounced in good responders. Plasma levels of pro-inflammatory cytokines decreased in all patients after

NACT. However, a high proportion of T cells in biopsies expressed immune checkpoint molecules PD-1 and CTLA4, and PD-L1 levels were significantly increased after NACT.

Conclusions

NACT may enhance host immune response but this effect is tempered by high/increased levels of PD-1, CTLA4 and PD-L1. Sequential chemo-immunotherapy may improve disease control in advanced HGSC.

Introduction

The aim of this study was to determine the influence of neoadjuvant chemotherapy, NACT, on the immune microenvironment in peritoneal metastases of high-grade serous ovarian cancer, HGSC. Early peritoneal and pleural spread is a feature of HGSC with a majority of patients presenting with FIGO stage IIIC and stage IV disease (1).

Platinum-based chemotherapy is the only backbone medical first line treatment approved for HGSC in the past thirty years and although most patients respond initially, resistance eventually develops in a majority of them. Peritoneal metastases are frequently the site of relapse and eventually lead to bowel obstruction that contributes to death in many patients (2,3).

In patients with Stage IIIC or IV disease who are not suitable for primary debulking surgery (PDS), three cycles of platinum-based NACT followed by interval debulking surgery (IDS) and adjuvant chemotherapy is an accepted alternative approach. This is equally effective while potentially associated with lower morbidity (4,5) although there is a need for international consensus criteria for patient selection in this approach.

There is good evidence that HGSC has potential to be an immunogenic tumor and activated T cells have been characterized in the tumor microenvironment and ascitic fluid (6) (7). There is an association between increased tumor-infiltrating leukocyte, TIL, density and longer survival (8,9) and TIL sub populations recognize shared tumor antigens, gene products from somatic mutations, as well as amplified or aberrant genes (10,11). Mutation frequency also correlated with an immune cell cytolytic activity transcriptional signature in ovarian cancer databases (12). However, TIL in HGSC biopsies are often suppressed or functionally exhausted, and immunotherapies, until

recently, not yet had a major impact on patients with advanced chemo-resistant disease (10,11,13).

Recent studies in animal cancer models have shown how the immune system plays an important role in the response to some cancer chemotherapies, inducing an 'immunogenic' cell death, presentation of neoantigens and an increase in acute inflammatory and tumor-destructive responses (14-16). Furthermore, recent mouse cancer experiments showed the efficacy of blocking the PD-1/PD-L1 axis following paclitaxel chemotherapy (17). The ability to sample HGSC biopsies at diagnosis and after NACT during surgery, gives us an opportunity to ask if similar responses occur in a clinical setting and if they do, whether this provides a rationale for introducing immunotherapy after NACT rather than in relapsed disease. We therefore studied a cohort of fifty-four women with stage IIIC and stage IV HGSC receiving NACT, as well as six women who underwent surgery before chemotherapy. Using transcriptional and protein analyses of prospectively collected metastatic peritoneal (omental) specimens, as well as plasma samples, we investigated the effects of platinum-based NACT on the immune microenvironment in patients and compared this to their response to chemotherapy as assessed by a recently published prognostic histologic score (18).

Materials and Methods

Patients and samples

Institutional review board approval was granted for the Barts Gynae Tissue Bank to collect and store biological material and clinical information. Patients were treated at St Bartholomew's Cancer Centre between 2010 and 2015 and gave written informed consent. Clinical parameters were collected using tissue repository databases and chart review.

Omental metastases and plasma samples from fifty-four FIGO stage IIIC and IV HGSC patients were collected prospectively before and after platinum-based neoadjuvant chemotherapy (details of patients and treatment are shown in Supplementary Table 1) and analysed in immunohistochemical, flow cytometric and transcriptomic experiments. Surgery was usually performed between three and four weeks after the last NACT. Samples from an additional six patients with FIGO stage IIIC and IV HGSC who underwent primary debulking surgery were used in the flow cytometry and RNAseq studies described below (Supplementary Table 2). These samples were matched to the NACT cohort in terms of amount of tumor and stroma in the biopsy, pre-treatment levels of plasma cytokines, age and stage. Inflammatory cytokine levels were measured in paired pre and post NACT plasma samples of twenty-three patients and twenty-two plasma samples were from healthy female volunteers (median age 47.5y, range 32 - 64). Supplementary Table 3 lists the numbers of samples that were used in each of the analyses.

The response to chemotherapy was assessed in IDS biopsies using a chemotherapy response score (CRS) that separates the patients into three major subgroups (18). CRS1 samples show minimal response to chemotherapy, CRS2,'poor' responders,

have easily identifiable malignant cells in the omentum after NACT and CRS3, 'good' responders, usually show extensive regression-associated fibro-inflammatory changes with absent or minimal numbers of malignant cells (18).

Formalin-fixed paraffin embedded (FFPE) tumor biopsies

Pre-treatment omental or peritoneal biopsies were obtained at diagnostic laparoscopy or diagnostic core biopsy. Sections of 4μm thickness were mounted on glass slides.

Blocks of omentum removed at interval debulking surgery after neoadjuvant chemotherapy, were reviewed by a pathologist according to ICCR guidelines (19). Blocks representing the area of worst response were selected and used to construct tissue microarrays (TMA) with a 1mm core size and up to 6 cores per patient sample.

Fresh tumor biopsies

Omental biopsies were collected in the operating theatre from untreated patients undergoing primary debulking surgery, PDS or diagnostic laparoscopy and from patients undergoing interval debulking surgery after NACT and fresh-frozen samples were histologically matched to FFPE specimens of the same patient by H&E review.

Blood samples

Sodium heparin blood (BD Vacutainer Systems) was immediately placed on ice within one week before NACT and within two weeks before IDS. The minimum time after the last cycle of chemotherapy was three weeks. Following centrifugation plasma from patients and controls was snap frozen and stored at -80°C.

Extraction of stroma vascular fraction

Fresh omental biopsies were subjected to mechanical dissection and enzymatic treatment. Briefly, the tissue was dissected with a scalpel, incubated in RPMI medium (Gibco) containing 5% FBS, 1mg/ml Collagenase D from *clostridium histolyticum*

(Roche) and 25µg/ml DNAse (Roche) at 37°C under agitation for 40min. The extract was then filtered through a 70µm pore strainer; red blood cells were lysed (eBioscience) and the Stroma Vascular Fraction (SVF) was frozen for later FACS analyses or freshly re-stimulated in vitro for intra-cellular cytokine staining.

Flow cytometry analyses

SVFs and peripheral blood mononuclear cells (PBMCs) were stained for flow cytometry analyses in PBS containing 2.5% BSA and 2mM EDTA for 30min at 4˚C. The following markers were used: CD45 APC efluor780 (eBioscience), CD3 BV650 (Biolegend), CD3 PE (eBioscience), CD4 PerCP-Cy5.5 (eBioscience), CD8 APC (eBioscience), CD8 FITC (eBioscience), PD-1 BV421 (Biolegend), CTLA4 PE (Biolegend), CD69 APC (eBioscience), CD25 PECy7 (eBioscience). Viability of the cells was assessed by staining with the fixable viability dye (FVD) eFluor506 (eBioscience) or DAPI (Sigma). Appropriate Fluorescence Minus One (FMO) controls were used in these experiments. Staining for $Foxp3^+$ T regulatory cells was performed using the Human Treg Kit (eBioscience) containing CD45 eFluor 780, CD4 FITC/CD25 APC, FOXP3 PE and the isotype control for Foxp3. Viability of the cells was assessed with FVD eFluor450 (eBioscience).

To study the production of IL-10 and IFNγ by omental T cells from pre and post treatment patients, 2.5 10^6 cells from the extracted SVF were re-stimulated in vitro in RPMI 10% FBS, 50ng/mL phorbol 12-myristate 13-acetate (PMA) (Sigma) and 1µg/mL Ionomycin (Sigma) for 5h at 37˚C, 5% CO_2. After the first hour of re-stimulation 10µg/ml Brefeldin A (Sigma) were added to the culture. Following re-stimulation, cells were stained for CD4 PerCP-Cy5.5 (eBioscience), CD8 FITC (eBioscience) and FVD 450 (eBioscience) in PBS 2.5% BSA + 2mM EDTA for 20min at 4˚C. Cells were then

washed, fixed for 20min at room temperature with the Fixation Buffer (eBioscience), permeabilized with the Permeabilization Buffer (eBioscience) and stained with anti-human IL10 PE (eBioscience) and IFNγ PECy7 (eBioscience) for 20min at room temperature. Corresponding isotype controls for IL10 and IFNγ were used to generate FMO controls. Stained samples were analysed using a LSRFortessa cell analyser (BD Biosciences) and data were analysed with FlowJo 9.4.6 (Treestar Inc.).

Immunohistochemistry

FFPE-embedded tissue sections were dewaxed and rehydrated. Antigen retrieval was performed using a pressure cooker and a citrate based antigen unmasking solution (Vector Laboratories) followed by staining in an autostainer (Dako) using an ultrasensitive HRP Polymer Kit (Biogenex). The following antibodies were used: CD8 clone C8/144B (Dako), FOXP3 clone 236A/E7 (abcam), CD45RO clone UCLH (Dako), PD-L1 clone SP142 (Spring Bioscience/Roche). Negative controls were isotype matched.

Immune cell quantification on digitalized slides

Immunohistochemically stained slides were scanned at 20x with a Pannoramic Flash Scanner (3D Histech). Images of 5 areas representing the entire biopsy of paired pre-post NACT samples were taken with an area of 0.58mm^2 per high-power field (Pannoramic software, 3D Histech). Intra-epithelial cells (within tumor islets) and intra-stromal cells were counted independently by three investigators, including one histopathologist, blinded for clinical information. Each HPF was scored as 0, 1+, 2+, 3+ or 4+ for tumor (within or direct contact with the epithelial component) and stromal regions. The cut-off was based on the typical density of these cell populations in HGSC omentum and prior joint discussion of the investigators (CD8 and CD45RO: no cells, 1-

10, 11-60, 61-150, >150 per HPF, respectively. FOXP3: no cells, 1-10, 11-40, 41-100, >100 per HPF respectively). The average score of all HPFs of one slide of one investigator was added to the corresponding scores of the other two and then divided by three.

Scoring of PD-L1 expression

PD-L1 was scored by a study pathologist using the criteria described in (20). Briefly, samples were scored for PD-L1 expression on tumor-infiltrating immune cells, which included macrophages, dendritic cells and lymphocytes. Specimens were given a score of 0-3 if <1%, 1-<5%, 5-<10% and ≥10% of cells were positive for PD-L1.

Plasma cytokine analysis

Cytokines were measured by electrochemiluminescence multiplex assay (V-Plex, MSD) on a Sector Imager (MSD) according to the manufacturers' protocol. The detection range for the assays was as follows: TNFα: 0.076pg/ml to 311 pg/ml; IL8: 0.133 pg/ml to 546pg/ml; IL6: 0.369pg/ml to 749pg/ml; IFNγ: 0.369pg/ml to 1510pg/ml; IL10: 0.076pg/ml to 313pg/ml; IL17: 1.38pg/ml to 5670pg/ml.

RNA isolation

Total RNA was isolated from frozen whole tissue using the RNeasy kit (Qiagen) following the manufacturers' instructions. Briefly, whole tissue was homogenized in RLT lysis buffer, passed through a QIAshredder (Qiagen) then purified on the mini spin columns, including the on-column DNAse treatment to remove any remaining DNA. The purified total RNA was then analyzed by Bioanalyzer 2100 expert (Agilent) as per manufacturers' instructions. RIN numbers between 9.9 and 8.0 were obtained.

Transcriptomic analysis

RNA Sequencing was performed by Oxford Gene Technology (Begbroke UK) using the Illumina HiSeq2500 platform and generated ~42 million 101 Base-pair paired end reads per sample. Sequenced reads were mapped to Human RefSeq genes archived in the Illumina iGenomes resource (http://support.illumina.com/sequencing/sequencing_software/igenome.html) using RSEM (21)(version 1.2.4) in dUTP strand-specific mode. As part of the RSEM pipeline, bowtie (version 0.12.7) (22) was used to perform the mapping stage. Subsequent mapped read counting was performed using RSEM. Differentially expressed genes were identified with the EdgeR package (23) using Bioconductor (version 2.7; www.bioconductor.org), running on R (version 2.12.1;R-REF). Genes with logCPM > 0 and FDR <0.05 were judged to be differentially expressed. Immunologic signatures that represent cell states and perturbations within the immune system were extracted from Msigdb (24) and used to perform GSEA with default settings comparing pair-wise comparisons. GSEA analysis on pre and post NACT samples, were interrogated using the MSigDB C7 immunologic collection available from the Broad Institute. This consisted of 1910 signatures, which comprise approximately 200 genes per signature. Signatures were considered significant if the corrected FDR *q* value was <0.05. Heatmaps shown in figures 3 and 4 are truncated to show only the genes identified as contributing to the enrichment score.

Data and materials availability

FASTQ data files supporting the RNASeq analysis have been uploaded to NCBI GEO database GSE71340.

Statistical analysis

For continuous variables that were approximately normally or normally distributed, mean and standard error of the mean are shown and t-test was conducted. For ordinal variables Mann Whitney test or Wilcoxon matched-pairs signed rank test were applied and Kruskal-Wallis test was used in addition to perform multiple group comparisons. Progression-free survival (PFS) was calculated from the date of first neoadjuvant chemotherapy to progression or death (whichever came first) using GCIG CA-125 criteria for biochemical progression. Overall survival (OS) was calculated from the date of first neoadjuvant chemotherapy to death from HGSC. Survival functions were estimated using the Kaplan-Meier method and the log-rank test was applied.

Results

Response to chemotherapy in the study cohort

Samples from a total of fifty-four patients receiving NACT and six patients who had surgery prior to chemotherapy were used in the experiments in this paper. Supplementary Table 3 summarizes the sample numbers used in each set of experiments. As described above, the response to chemotherapy was assessed in the interval debulking, IDS, biopsies using the CRS (18). CRS1 samples show minimal response to chemotherapy, CRS2,'poor' responders, have easily identifiable malignant cells in the omentum after NACT and CRS3, 'good' responders, usually show extensive regression-associated fibro-inflammatory changes with absent or minimal numbers of malignant cells (18). None of the IDS samples in our experiments, by chance and due to prevalence, scored as CRS1. 'Good responder' patients with samples scored as CRS3 had significantly improved progression-free survival (p=0.002) and overall survival (p=0.03) compared to 'poor responder' patients whose biopsies scored as CRS2 (Supplementary Figure 1).

T cell density pre and post NACT

From twenty-five of the HGSC patients described above, we obtained matched omental biopsies taken at pretreatment and at IDS. Using immunohistochemistry, the biopsies were stained for $CD8^+$ T cells, $CD45RO^+$ memory cells and $Foxp3^+$T regulatory cells. Figure 1 and Supplementary Figure 2 show the cell density in malignant cell areas and adjacent stromal areas. Pretreatment, there was no difference in the density of cells positive for the above markers between CRS2 'poor' and CRS3 'good' responders. After NACT there were still marked infiltrates of $CD8^+$ T cells and $CD45RO^+$ memory cells in the stroma and again no difference between CRS2 or CRS3 biopsies. $CD8^+$ T cells and

$CD45RO^+$ memory cells in the malignant cell areas of CRS2 biopsies remained at high levels; in fact $CD8^+$ cell density increased in approximately 50% of patients and the tumor:stroma ratio of $CD8^+$ and $CD45RO^+$ cells in individual patients was essentially unchanged pre and post chemotherapy in the CRS2 biopsies (Supplementary Figure 3).

In contrast, there was a significant decline in the density of $Foxp3^+$ cells in the stromal areas of the CRS3 'good' responder biopsies after NACT (p=0.02) but there was no significant change in the CRS2 biopsies (Figure 1). As Foxp3 is a marker of immunosuppressive T regulatory cells, we next asked whether NACT increased T cell activation.

Evidence for T cell activation after NACT

We assessed the phenotype of the T cells in the HGSC omental metastases by flow cytometry analysis of tumor-infiltrating leukocytes from twenty-two of the HGSC biopsies. As it was not possible to obtain sufficient material for flow cytometry from diagnostic biopsies for pretreatment samples in these experiments, to assess pretreatment T cell phenotypes we used six samples obtained at primary debulking and two laparoscopic biopsies obtained before NACT. In agreement with the results in Figure 1, the percentage of $CD3^+$ cells in the $CD45^+$ leukocyte population did not change pre or post NACT, irrespective of response to chemotherapy (Figure 2A). Likewise there were no significant changes in $CD8^+$, $CD4^+$ T cells or CD4:CD8 ratio (Figure 2B-D). A subpopulation of the $CD4^+$ T cells was $CD25^+$ $Foxp3^+$ suggesting they were T-regulatory cells. When comparing CRS2 and CRS3 patients we observed a decrease in the percentage of $CD4^+$ T cells that were $CD25^+Foxp3^+$ in the CRS3 biopsies (p=0.015, Mann-Whitney test) (Figure 2E), again supporting the results in Figure 1. The ratio of $CD4^+CD25^+$ $Foxp3^+$ cells to $CD4^+CD25^+Foxp3^-$ cells also

decreased in post NACT CRS3 and CRS2 biopsies compared to pre-treatment, and the difference between CRS2 and CRS3 was significant (p=0.03, Mann-Whitney test) (Figure 2F). When applying a correction for multiple group comparison, the differences were not deemed significant (p=0.06 (Figure 2E) and p=0.09 (Figure 2F), Kruskal-Wallis test).

We next studied the functional ability of the T cells in the biopsies to produce IFN-γ as a marker of T cell activation and anti-tumor response, and IL-10 as a marker of immunosuppression. Cells extracted from eleven HGSC omental samples, as well as peripheral blood mononuclear cells, PBMCs, from healthy control women (n=3-5), were stimulated *in vitro* and then stained for intracellular IFNγ and IL-10 (Figure 2G, H). A significantly higher proportion of omental $CD4^+$ and $CD8^+$ T cells were able to produce IFNγ compared to peripheral T cells from healthy controls. When compared to pre treatment biopsies, post NACT CRS3 patients had a significantly higher proportion of $IFN\gamma^+$ $CD4^+$ T cells (p=0.002, Figure 2G). No significant difference in the proportion of IL10 producing $CD4^+$ and $CD8^+$T cells was observed between pre and post NACT samples (Figure 2G, H).

Gene set enrichment analysis of immune gene signatures pre and post NACT

We extracted total RNA from twenty of the HGSC omental metastasis biopsies for which we had sufficient material and analysed gene expression by RNAseq. Nine samples were from CRS3 good responders post NACT and seven from CRS2 poor responders. For pre-treatment samples we used two biopsies from stage IIIC or IV HGSC patients undergoing primary debulking surgery and two biopsies obtained from patients before NACT as described for Figure 2. Gene set enrichment analysis (GSEA) was conducted Changes to immune cell phenotypes from both the adaptive and innate pathways were

seen when comparing CRS3 to CRS2 samples, and individually (CRS2 or CRS3) to Pre NACT samples. In particular changes associated with T-cell phenotype were found to have the highest significance (lowest FDR value). In agreement with the results in Figures 1 and 2, we found that the FOXP3-associated T regulatory cell gene signatures were differentially regulated in pre versus post NACT patients. FOXP3 regulated genes whose expression is decreased following differentiation to a T regulatory phenotype (25) were enriched in pretreatment versus both CRS2 and CRS3 post NACT biopsies (Figure 3A and B). We also observed an enrichment of this gene signature in CRS2 poor responder biopsies compared to CRS3 biopsies (Figure 3C).

Further GSEA analysis revealed an increase in expression of T-helper 1 (Th1)-associated genes after NACT in both poor (CRS2) and good (CRS3) responders (Figure 4A, 4B). The gene set used contained genes that were experimentally up-regulated when naïve T-cells were activated to a Th1 phenotype in vitro (26). We also noted that the Th1 phenotype was enriched in CRS3 patients compared to CRS2 (Figure 4C). Meta analysis of TCGA data has identified GZMA (encoding granzyme A) and PRF1 (encoding perforin 1) as specifically co-expressed by cytotoxic T-cells (12). We compared gene expression levels for both markers within our data set (Figure 4D-F). There was a tendency for both genes to be upregulated in the post NACT versus pretreatment samples and the difference with PRF1 was significant p=0.03 (Figure 4D,E). The geometric mean of both genes (Figure 4F) again showed a tendency towards upregulation post-NACT. These experiments suggest that NACT reduced T regulatory cell activity in HGSC metastases while increasing T cell activation and Th1 responses and these effects were most profound in the CRS3 good responder patients.

We next asked if the potential for efficient host anti-tumor immune responses was influenced by immune checkpoint molecules.

The effect of NACT on immune checkpoint molecules

More than 60% of $CD4^+$ and $CD8^+$ T cells in omental metastases from six pre and sixteen post NACT patients expressed the immune checkpoint molecule programmed cell death-1 (PD-1) as assessed by flow cytometry (Figure 5A and B). Between 15 and 30% of the $CD4^+$ cells and 5 to 10% of the $CD8^+$ cells expressed cytotoxic T-lymphocyte-associated protein 4, CTLA4, in twenty-two biopsies (Figure 5C and D) and most of the $CTLA4^+$ T cells co-expressed PD-1 (Figure 5E and F).

Immunohistochemistry staining showed that the PD-1 ligand PD-L1 was frequently associated with the immune cell compartment of the HGSC tumor microenvironment. Using an antibody developed for anti-PD-L1 clinical trials (clone SP142) and a scoring method on immune cells (20) we found that PD-L1 protein was significantly increased in post NACT compared to pre NACT biopsies irrespective of response to treatment in paired pre- and post NACT biopsies of twenty-six patients ($p=0.03$, Figure 5F, G and Supplementary Figure 4). Hence, potential beneficial effects of chemotherapy in stimulating T cell activation might be impaired by the high expression of immune checkpoint molecules.

Plasma levels of cytokines

Cancer-related inflammatory pathways can also contribute to the immune suppressive tumor microenvironment (27) and ovarian cancers have complex tumor-promoting inflammatory cytokine networks (28) that can be reflected by increases in systemic cytokine levels (29). We measured key cytokines implicated in tumor-promoting inflammation, as well as T cell activation and immune suppression, in forty-six matched

pre and post NACT plasma samples from twenty-three patients. Levels of three major inflammatory cytokines with potential tumor-promoting activity, TNF, IL-8 and IL-6, significantly decreased after NACT ($p=0.0008$, $p=0.001$ and $p=0.0006$, respectively, Figure 6A-C). All plasma levels were elevated pre-treatment but post NACT levels were not statistically different from values obtained from twenty-two healthy females. There were no differences between patients whose samples were scored CRS2 and CRS3.

In contrast, plasma IFNγ was increased in post treatment patients compared to healthy controls ($p=0.005$) with a trend towards an increase post-treatment versus pre-treatment (Figure 6D). Pre-treatment patient plasma IL-10 levels were significantly higher compared to controls before NACT ($p=0.04$) and decreased after NACT ($p<0.001$ (Figure 6E). IL-17 levels were significantly elevated in HGSC patients compared to controls ($p=0.006$) and remained elevated after NACT ($p=0.02$, Figure 6F).

Discussion

As well as in malignant melanoma, there have been some encouraging responses to immune checkpoint inhibitor therapy in patients with difficult-to treat metastatic solid cancers such as non-small cell lung cancer (30), bladder cancer (20) and ovarian cancer (13). However many patients show no benefit, not all cancer types respond and most trials are conducted after multiple treatments and with drug-resistant disease. The hypothesis of our study was that immunotherapies such as immune checkpoint blockade may result in enhanced clinical benefit if given after or during first line chemotherapy. The NACT protocols used for many patients with stage IIIC and stage IV HGSC gave us an opportunity to investigate this in a clinical setting.

We believe that this is the first in-depth analysis of the effects of first-line chemotherapy on a human metastatic tumor microenvironment. We demonstrate that NACT induces activation of $CD4^+$ T-cells and that $CD8^+$ T cells and $CD45RO^+$ memory cells are present in omental metastases after NACT. By incorporating a recently developed prognostically significant histological score (18) we show that omental metastases biopsies from patients with good response (CRS3) to NACT have more pronounced T-cell activation and reduced T regulatory cell infiltration compared to poor responders (CRS2). Importantly, even those patients who had a poor response to three cycles of platinum-based chemotherapy had high densities of $CD8^+$ T cells and $CD45RO^+$ memory cells and their ability to produce IFNγ was preserved. Moreover, increased levels of transcripts coding for cytotoxic markers post-NACT suggested chemotherapy might enhance the cytotoxicity of immune effector cells, such as CD8+ T cells and NK cells towards the tumor. These local changes were accompanied by a decline, usually back to healthy control values, in systemic levels of cytokines implicated in cancer-

related inflammation in all patients. The potential enhancement of host anti-tumor immune response and reduction in mediators of cancer-related inflammation was tempered by the fact that levels of the immune-checkpoint molecules PD-1 and CTLA4 on $CD4^+$ and $CD8^+$ T-cells remained high after NACT. Levels of PD-L1 ligand on tumor-infiltrating immune cells were significantly increased. The fact that the immune checkpoint targets are present or increased after NACT, in the presence of significant densities of $CD8^+$ T cells and memory cells provides a rationale for cancer immunotherapy, especially immune checkpoint blockade, in the HGSC first line setting at this early time point. The presence or absence of T-cells in solid tumors is a key limiting factor for cancer immunotherapy (31) and the presence of $CD8^+$ T cells at the invasive margin was predictive of response to anti PD-1 treatment in malignant melanoma (32).

There is already some evidence that prior chemotherapy enhances the effect of immunotherapy. Successful responses to adoptive therapy with CAR T cells, TCR T cells, and TILs are regularly seen in cancer patients who have become chemotherapy-resistant. In terms of ovarian cancer, there were responses to interleukin-2 immunotherapy in patients who had become resistant to platinum therapy (33), while in a first-line study chemotherapy plus IFNγ 1-b immunotherapy showed a decreased OS compared to chemotherapy alone (34). This highlights the need for careful monitoring of patients during combination chemotherapy.

The relative contribution of platinum versus taxane to the immunostimulatory effects seen in our study is an open question because almost all patients received the combination therapy. Experimental studies suggest that cisplatin does not induce immunogenic cell death (ICD) (35) but carboplatin and docetaxel produce partial

features of ICD (36). Chemotherapy can also activate the host immune system by several other mechanisms (37) such as increased presentation of neo-antigens. Chemotherapy before immunotherapy is of particular interest since efficacy of PD-1 blockade has recently been shown to correlate with neoantigen burden in non-small cell lung cancer (38).

In ovarian cancer there are conflicting results relating to the prognostic impact of T regulatory cells (39,40). Our data obtained at transcriptional, protein and cellular level show a reduced T regulatory cell signature and density after NACT is most apparent in biopsies of tumors classified as CRS3 good responders, providing evidence for a link between chemotherapy efficiency and Treg density. In addition to reduced Tregs after NACT in good responders we have observed by flow cytometry a shift of the $Foxp3^-$ population towards increased CD25 expression, again most pronounced in good responders. This population has been shown to have an 'exhausted' phenotype that could effectively been reversed using an anti-PD-1 monoclonal antibody (41). We suggest that blocking the PD-1/PD-L1 axis is a way to inhibit T regulatory cell function and enhance the antitumor-effectiveness of the $CD4^+CD25^+$ T cells. Future work in larger cohorts may reveal insights into functionally different subsets of T regulatory cells with potentially different prognostic and predictive value (42) (43).

There is much evidence that cancer-related inflammation is also tumor-promoting (44) although clinical trials that target inflammatory mediators or cells are not as advanced as some other immunotherapy approaches (27) (34). As the adaptive immune response is heavily dependent on innate immunity, inhibiting some of the tumor-promoting immunosuppressive actions of the innate immune system might enhance the potential of immunotherapies that activate a nascent antitumor response. It is therefore

encouraging that NACT had a significant impact on systemic levels of three key inflammatory cytokines in our study. TNF and IL-6 are major players in the complex cytokine networks that drive tumor progression in ovarian cancer (28,29,45). Elevated IL-6 produced by malignant cells was a cause of paraneoplastic thrombocytosis in HGSC patients (29) and plasma IL-8 correlated with tumor burden and treatment response across a range of human and experimental cancers (46). The observation that all three cytokines decrease to normal plasma levels after NACT further suggests that this is a favorable time to introduce immunotherapy, taken with the finding of an increase in the Th1 cytokine IFNγ in the patient plasma.

In summary, we have been able to study the human tumor microenvironment at the transcriptomic, proteomic and cellular level at a key site of cancer dissemination and under conditions that reflect current practice of patient care – the disease at diagnosis and after NACT. Our results suggest that NACT opens a window of opportunity for immunotherapies such as immune checkpoint blockade for patients with different levels of response to chemotherapy. We conclude that incorporation of immunotherapies into post chemotherapy treatment options could be of benefit for prolonged disease control in patients with advanced HGSC and, if confirmed, in patients with other cancer types.

Acknowledgments

We thank the patients for donating samples to the Barts Gynae Tissue Bank and the doctors and nurses at St Bartholomew's Gynaecological Cancer Centre for their support. We are grateful to Dr Dhafir Al Okati, Queens Hospital, Romford and Dr Konstantinos Giaslakiotis, Whipps Cross University Hospital, London for providing biopsy samples for the study. We also wish to thank Dr Ian Said, Barts Health NHS Trust and George Elia, Andrew Owen and Dr Linda Hammond, Barts Cancer Institute for technical support.

References

1. Vaughan S, Coward J, Bast Jr RC, Berchuck A, Berek JS, Brenton JD, et al. Rethinking ovarian cancer: recommendations for improving outcomes. Nature Reviews Cancer 2011;11.
2. Tan DS, Agarwal R, Kaye SB. Mechanisms of transcoelomic metastasis in ovarian cancer. Lancet Oncol 2006;7(11):925-34.
3. Jayson GC, Kohn EC, Kitchener HC, Ledermann JA. Ovarian cancer. Lancet 2014;384(9951):1376-88.
4. Vergote I, Trope CG, Amant F, Kristensen GB, Ehlen T, Johnson N, et al. Neoadjuvant chemotherapy or primary surgery in stage IIIC or IV ovarian cancer. N Engl J Med 2010;363(10):943-53.
5. Kehoe S, Hook J, Nankivell M, Jayson GC, Kitchener H, Lopes T, et al. Primary chemotherapy versus primary surgery for newly diagnosed advanced ovarian cancer (CHORUS): an open-label, randomised, controlled, non-inferiority trial. Lancet 2015.
6. Ioannides CG, Platsoucas CD, Rashed S, Wharton JT, Edwards CL, Freedman RS. Tumor cytolysis by lymphocytes infiltrating ovarian malignant ascites. Cancer Res 1991;51(16):4257-65.
7. Kooi S, Zhang HZ, Patenia R, Edwards CL, Platsoucas CD, Freedman RS. HLA class I expression on human ovarian carcinoma cells correlates with T-cell infiltration in vivo and T-cell expansion in vitro in low concentrations of recombinant interleukin-2. Cellular immunology 1996;174(2):116-28.
8. Zhang L, Conejo-Garcia JR, Katsaros D, Gimotty PA, Massobrio M, Regnani G, et al. Intratumoral T cells, recurrence, and survival in epithelial ovarian cancer. The New England journal of medicine 2003;348(3):203-13.
9. Webb JR, Milne K, Watson P, Deleeuw RJ, Nelson BH. Tumor-infiltrating lymphocytes expressing the tissue resident memory marker CD103 are associated with increased survival in high-grade serous ovarian cancer. Clin Cancer Res 2014;20(2):434-44.
10. Nelson BH. New insights into tumor immunity revealed by the unique genetic and genomic aspects of ovarian cancer. Curr Opin Immunol 2015;33:93-100.
11. Zsiros E, Tanyi J, Balint K, Kandalaft LE. Immunotherapy for ovarian cancer: recent advances and perspectives. Curr Opin Oncol 2014;26(5):492-500.
12. Rooney MS, Shukla SA, Wu CJ, Getz G, Hacohen N. Molecular and genetic properties of tumors associated with local immune cytolytic activity. Cell 2015;160(1-2):48-61.
13. Hamanishi J, Mandai M, Ikeda T, Minami M, Kawaguchi A, Murayama T, et al. Safety and Antitumor Activity of Anti-PD-1 Antibody, Nivolumab, in Patients With Platinum-Resistant Ovarian Cancer. J Clin Oncol 2015; 33(34):4015-22
14. Vacchelli E, Aranda F, Eggermont A, Galon J, Sautes-Fridman C, Cremer I, et al. Trial Watch: Chemotherapy with immunogenic cell death inducers. Oncoimmunology 2014;3(1):e27878.
15. Menger L, Vacchelli E, Adjemian S, Martins I, Ma Y, Shen S, et al. Cardiac glycosides exert anticancer effects by inducing immunogenic cell death. Sci Transl Med 2012;4(143):143ra99.

16. Michaud M, Martins I, Sukkurwala AQ, Adjemian S, Ma Y, Pellegatti P, et al. Autophagy-dependent anticancer immune responses induced by chemotherapeutic agents in mice. Science 2011;334(6062):1573-7.
17. Peng J, Hamanishi J, Matsumura N, Abiko K, Murat K, Baba T, et al. Chemotherapy Induces Programmed Cell Death-Ligand 1 Overexpression via the Nuclear Factor-kappaB to Foster an Immunosuppressive Tumor Microenvironment in Ovarian Cancer. Cancer Res 2015;75(23):5034-45.
18. Bohm S, Faruqi A, Said I, Lockley M, Brockbank E, Jeyarajah A, et al. Chemotherapy Response Score: Development and Validation of a System to Quantify Histopathologic Response to Neoadjuvant Chemotherapy in Tubo-Ovarian High-Grade Serous Carcinoma. J Clin Oncol 2015;33(22):2457-63.
19. McCluggage WG, Judge MJ, Clarke BA, Davidson B, Gilks CB, Hollema H, et al. Data set for reporting of ovary, fallopian tube and primary peritoneal carcinoma: recommendations from the International Collaboration on Cancer Reporting (ICCR). Mod Pathol 2015;28(8):1101-22.
20. Powles T, Eder JP, Fine GD, Braiteh FS, Loriot Y, Cruz C, et al. MPDL3280A (anti-PD-L1) treatment leads to clinical activity in metastatic bladder cancer. Nature 2014;515(7528):558-62.
21. Li B, Dewey CN. RSEM: accurate transcript quantification from RNA-Seq data with or without a reference genome. BMC bioinformatics 2011;12:323.
22. Langmead B, Trapnell C, Pop M, Salzberg SL. Ultrafast and memory-efficient alignment of short DNA sequences to the human genome. Genome biology 2009;10(3):R25.
23. Robinson MD, McCarthy DJ, Smyth GK. edgeR: a Bioconductor package for differential expression analysis of digital gene expression data. Bioinformatics 2010;26(1):139-40.
24. Subramanian A, Tamayo P, Mootha VK, Mukherjee S, Ebert BL, Gillette MA, et al. Gene set enrichment analysis: A knowledge-based approach for interpreting genome-wide expression profiles. PNAS 2005;43:15545-50.
25. Hill JA, Feuerer M, Tash K, Haxhinasto S, Perez J, Melamed R, et al. Foxp3 transcription-factor-dependent and -independent regulation of the regulatory T cell transcriptional signature. Immunity 2007;27(5):786-800.
26. Abbas AR, Baldwin D, Ma Y, Ouyang W, Gurney A, Martin F, et al. Immune response in silico (IRIS): immune-specific genes identified from a compendium of microarray expression data. Genes and immunity 2005;6(4):319-31.
27. Crusz SM, Balkwill FR. Inflammation and cancer: advances and new agents. Nat Rev Clin Oncol 2015; 12(10): 584-596
28. Kulbe H, Chakravarty P, Leinster DA, Charles KA, Kwong J, Thompson RG, et al. A Dynamic Inflammatory Cytokine Network in the Human Ovarian Cancer Microenvironment. Cancer research 2012;72(1):66-75.
29. Stone RL, Nick AM, McNeish IA, Balkwill F, Han HD, Bottsford-Miller J, et al. Paraneoplastic thrombocytosis in ovarian cancer. The New England journal of medicine 2012;366(7):610-8.
30. Brahmer J, Reckamp KL, Baas P, Crino L, Eberhardt WE, Poddubskaya E, et al. Nivolumab versus Docetaxel in Advanced Squamous-Cell Non-Small-Cell Lung Cancer. N Engl J Med 2015;373(2):123-35.

31. Melero I, Rouzaut A, Motz GT, Coukos G. T-cell and NK-cell infiltration into solid tumors: a key limiting factor for efficacious cancer immunotherapy. Cancer Discov 2014;4(5):522-6.
32. Tumeh PC, Harview CL, Yearley JH, Shintaku IP, Taylor EJ, Robert L, et al. PD-1 blockade induces responses by inhibiting adaptive immune resistance. Nature 2014;515(7528):568-71.
33. Vlad AM, Budiu RA, Lenzner DE, Wang Y, Thaller JA, Colonello K, et al. A phase II trial of intraperitoneal interleukin-2 in patients with platinum-resistant or platinum-refractory ovarian cancer. Cancer Immunol Immunother 2010;59(2):293-301.
34. Alberts DS, Marth C, Alvarez RD, Johnson G, Bidzinski M, Kardatzke DR, et al. Randomized phase 3 trial of interferon gamma-1b plus standard carboplatin/paclitaxel versus carboplatin/paclitaxel alone for first-line treatment of advanced ovarian and primary peritoneal carcinomas: results from a prospectively designed analysis of progression-free survival. Gynecol Oncol 2008;109(2):174-81.
35. Martins I, Kepp O, Schlemmer F, Adjemian S, Tailler M, Shen S, et al. Restoration of the immunogenicity of cisplatin-induced cancer cell death by endoplasmic reticulum stress. Oncogene 2011;30(10):1147-58.
36. Bezu L, Gomes-de-Silva LC, Dewitte H, Breckpot K, Fucikova J, Spisek R, et al. Combinatorial strategies for the induction of immunogenic cell death. Frontiers in immunology 2015;6:187.
37. Inoue H, Tani K. Multimodal immunogenic cancer cell death as a consequence of anticancer cytotoxic treatments. Cell death and differentiation 2014;21(1):39-49.
38. Rizvi NA, Hellmann MD, Snyder A, Kvistborg P, Makarov V, Havel JJ, et al. Cancer immunology. Mutational landscape determines sensitivity to PD-1 blockade in non-small cell lung cancer. Science 2015;348(6230):124-8.
39. Curiel TJ, Coukos G, Zou L, Alvarez X, Cheng P, Mottram P, et al. Specific recruitment of regulatory T cells in ovarian carcinoma fosters immune privilege and predicts reduced survival. Nat Med 2004;10(9):942-9.
40. Leffers N, Gooden MJ, de Jong RA, Hoogeboom BN, ten Hoor KA, Hollema H, et al. Prognostic significance of tumor-infiltrating T-lymphocytes in primary and metastatic lesions of advanced stage ovarian cancer. Cancer Immunol Immunother 2009;58(3):449-59.
41. deLeeuw RJ, Kroeger DR, Kost SE, Chang PP, Webb JR, Nelson BH. CD25 identifies a subset of CD4(+)FoxP3(-) TIL that are exhausted yet prognostically favorable in human ovarian cancer. Cancer Immunology Research 2015;3(3):245-53.
42. Abbas AK, Benoist C, Bluestone JA, Campbell DJ, Ghosh S, Hori S, et al. Regulatory T cells: recommendations to simplify the nomenclature. Nat Immunol 2013;14(4):307-8.
43. Mantovani A, Allavena P, Sica A, Balkwill F. Cancer-related inflammation. Nature 2008;454:436-44.
44. Coward J, Kulbe H, Chakravarty P, Leader D, Vassileva V, Leinster DA, et al. Interleukin-6 as a Therapeutic Target in Human Ovarian Cancer. Clinical Cancer Research 2011;17(18):6083-96.

45. Sanmamed MF, Carranza-Rua O, Alfaro C, Onate C, Martin-Algarra S, Perez G, et al. Serum interleukin-8 reflects tumor burden and treatment response across malignancies of multiple tissue origins. Clin Cancer Res 2014;20(22):5697-707.

Figure Legends:

Figure 1. T cell density and location in matched pre- and post-treatment omental biopsies

Amount and localization of $CD8^+$ T-cells, $CD45RO^+$ memory cells and $Foxp3^+$ cells in omental metastasis in fifty matched pre and post chemotherapy peritoneal biopsies from twenty-five patients.

Analysis of cell amount pre- to post NACT based on a 5-tier score in tumor and stroma. Intratumoral cells post NACT in CRS3 good responders are 'not applicable' since no large tumor islets are left in the omentum after NACT in these patients. Note that all CRS2 biopsies post NACT were positive for intra-tumoral and intra-stromal $CD8^+$ and $CD45RO^+$ cells, in many samples increased compared to pre chemotherapy. $Foxp3^+$ T regulatory cells do not increase in tumor and stroma of CRS2 biopsies and decrease significantly in stroma of CRS3 biopsies (* = $p<0.05$).

Figure 2. Effect of NACT on the T cell populations in omental metastases

(A to D) Flow cytometry analysis of the percentage of $CD3^+CD4^+$ and $CD3^+CD8^+$ T cells in omental metastases from six pre and sixteen post-treatment patients according to response. (E) The percentage of $CD4^+CD25^+Foxp3^+$ T regulatory cells in omental metastases of six pre and sixteen post-NACT patients was analyzed by flow cytometry. (F) Shows the ratio of $CD4^+CD25^+Foxp3^+$ Tregs to $CD4^+CD25^+Foxp3^-$ T cells. (G and H) Cells extracted from eleven omental metastases (3 pre-treatment, 5 post-NACT CRS3 good responders and 3 post-NACT CRS2 poor responders) and healthy blood (n=3 to 5) were re-stimulated in culture with 50ng/ml PMA, 1µg/ml Ionomycin and 10µg/ml Brefeldin A for 5 hours and stained for the presence of intracellular IFNγ and

IL10 in $CD4^+$ and $CD8^+$ T cells. Not indicated in the figures: The percentage of $CD4^+IFN\gamma^+$ and $CD8^+IFN\gamma^+$ cells was significantly higher in pre and post treatment omental metastases compared to control blood ($p< 0.001$); the percentage of $CD4^+IL10^+$ and $CD8^+IL10^+$ cells was significantly higher in metastases from CRS3 patients compared to control blood ($p<0.05$). All other significant results indicated with * = $p<0.05$ and ** = $p<0.01$.

Figure 3. Gene expression analysis of Treg signature pre and post NACT

GSEA analysis of twenty samples using a set of genes down regulated on conversion of a naïve T cell to a Treg phenotype compared against a FOXP3 mutant T-cell line (25). Red squares indicate genes of the core enrichment, shown in the corresponding heatmap. A) Pre vs Post CRS3 good responders, FDR < 0.0001, B) Pre vs Post CRS2 poor responders, FDR <0.0001 and C) Post CRS3 vs Post CRS2, FDR = 0.009.

Figure 4. Gene expression analysis of T-cell responses to NACT

(A-B) GSEA Th1 signature generated from naïve T-cells that have been activated to a Th1 phenotype in vitro (26) is enriched after NACT in (A) CRS2 poor responders (FDR = 0.02) and (B) CRS3 good responders (FDR = 0.004) compared to pre-treatment and (C) the same signature compared between good and poor responders to NACT (FDR = 0.014). Red squares indicate genes of the core enrichment, shown in the corresponding heatmap. D) and E) transcripts per million (TPM) of PRF1 and GZMA expression between Pre and Post NACT samples, and F) the geometric mean of PRF1 and GZMA expression compared between Pre and Post NACT samples. (* = $p<0.05$)

Figure 5. Expression of checkpoint molecules in omental metastasis before treatment and according to response to chemotherapy

(A to F) Expression of PD-1 and CTLA4 on $CD4^+$ and $CD8^+$ T cells assessed on twenty-two samples separated into pre-treatment and post NACT according to CRS scores. (G) Examples of positive staining for PD-L1 before and after NACT (IHC, antibody clone SP142), (H) Analysis of IHC staining for PD-L1 positive immune cells in fifty-two paired samples before and after NACT. (* = $p<0.05$)

Figure 6. Systemic cytokine levels before and after neoadjuvant chemotherapy.

(A to F) Systemic levels of TNF (A), IL-8 (B), IL-6 (C), IFNγ (D), IL-10 (E) and IL17 (F) in fourty-six paired pre and post NACT plasma samples of twenty-three patients and of twenty-two healthy female controls (IL-17: ten controls) measured by electrochemoluminescence multiplex assays. (* = $p<0.05$; ** = $p<0.01$).

Figures:

Figure 1

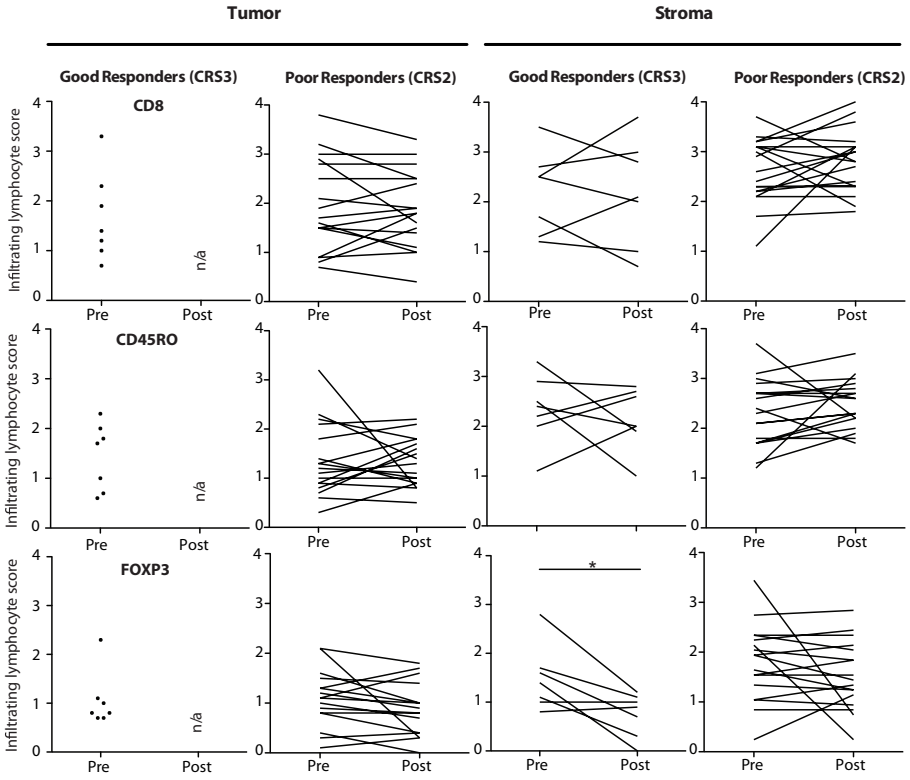

Figure 2

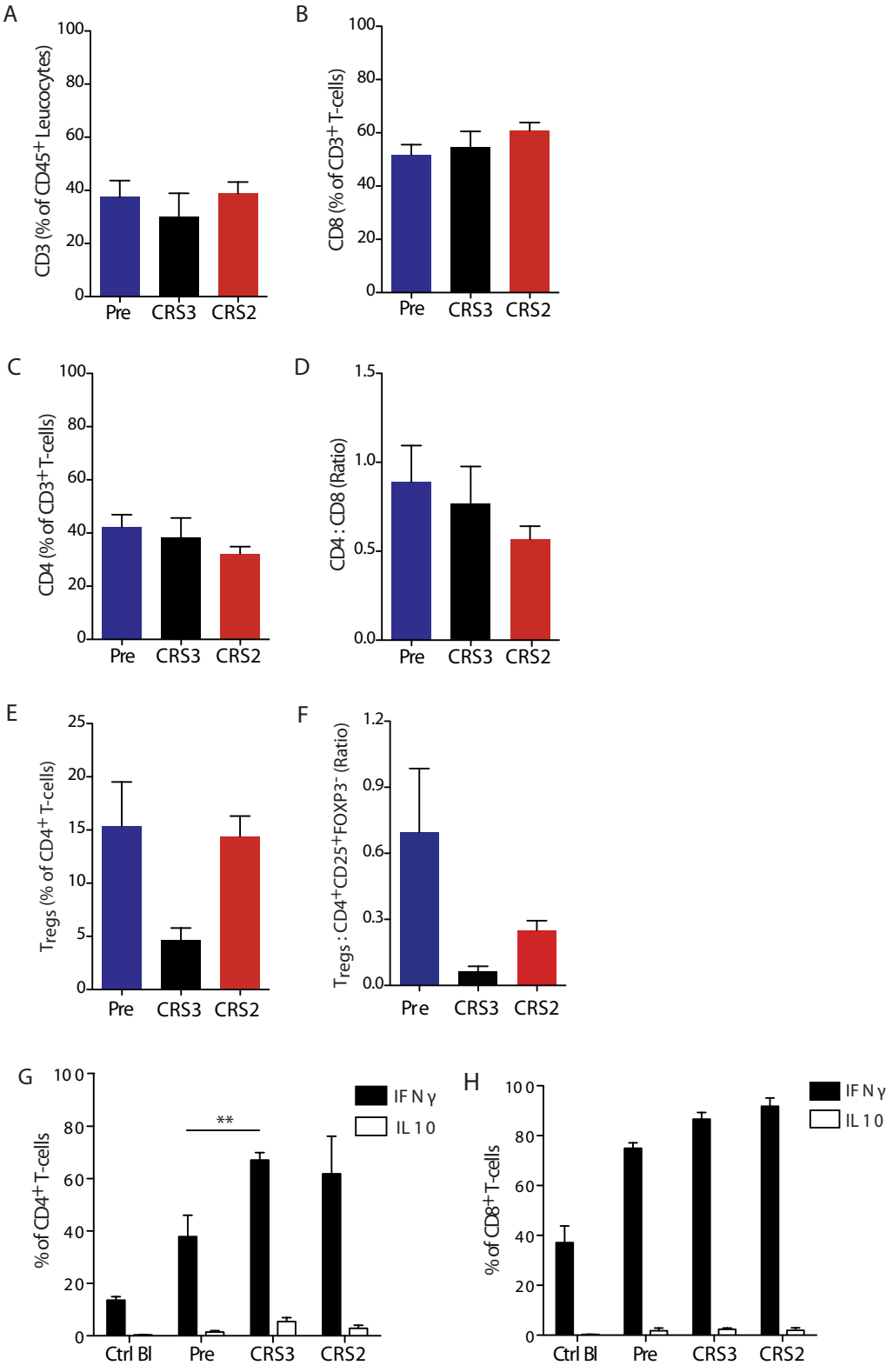
A
CD3 (% of CD45+ Leucocytes)
100
80
60
40
20
0
Pre
CRS3
CRS2
B
CD8 (% of CD3+ T-cells)
100
80
60
40
20
0
Pre
CRS3
CRS2
C
CD4 (% of CD3+ T-cells)
100
80
60
40
20
0
Pre
CRS3
CRS2
D
CD4 : CD8 (Ratio)
1.5
1.0
0.5
0.0
Pre
CRS3
CRS2
E
Tregs (% of CD4+ T-cells)
25
20
15
10
5
0
Pre
CRS3
CRS2
F
Tregs : CD4+CD25+FOXP3- (Ratio)
1.2
0.9
0.6
0.3
0.0
Pre
CRS3
CRS2
G
% of CD4+ T-cells
100
80
60
40
20
0
**
IFNγ
IL10
Ctrl Bl
Pre
CRS3
CRS2
H
% of CD8+ T-cells
100
80
60
40
20
0
IFNγ
IL10
Ctrl Bl
Pre
CRS3
CRS2

Figure 3

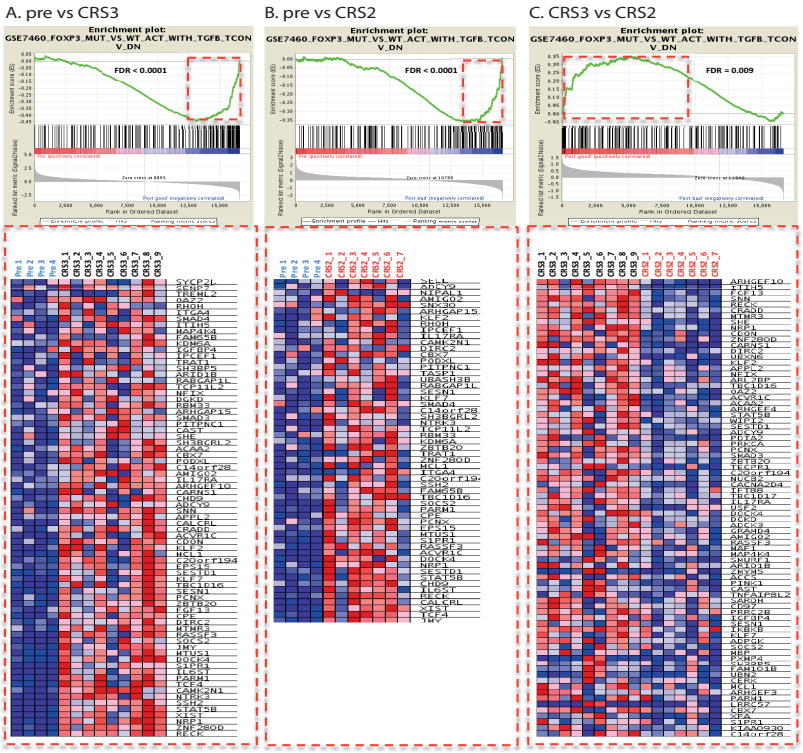
A. pre vs CRS3
B. pre vs CRS2
C. CRS3 vs CRS2
Enrichment plot:
GSE7460_FOXP3_MUT_VS_WT_ACT_WITH_TGFB_TCON
V_DN
FDR < 0.0001
FDR < 0.0001
FDR = 0.009
Rank in Ordered Dataset
Pre 1
Pre 2
Pre 3
Pre 4
CRS3_1
CRS3_2
CRS3_3
CRS3_4
CRS3_5
CRS3_6
CRS3_7
CRS3_8
CRS3_9
CRS2_1
CRS2_2
CRS2_3
CRS2_4
CRS2_5
CRS2_6
CRS2_7
CRS2_4
CRS2_5
CRS2_6
CRS2_7

Figure 4

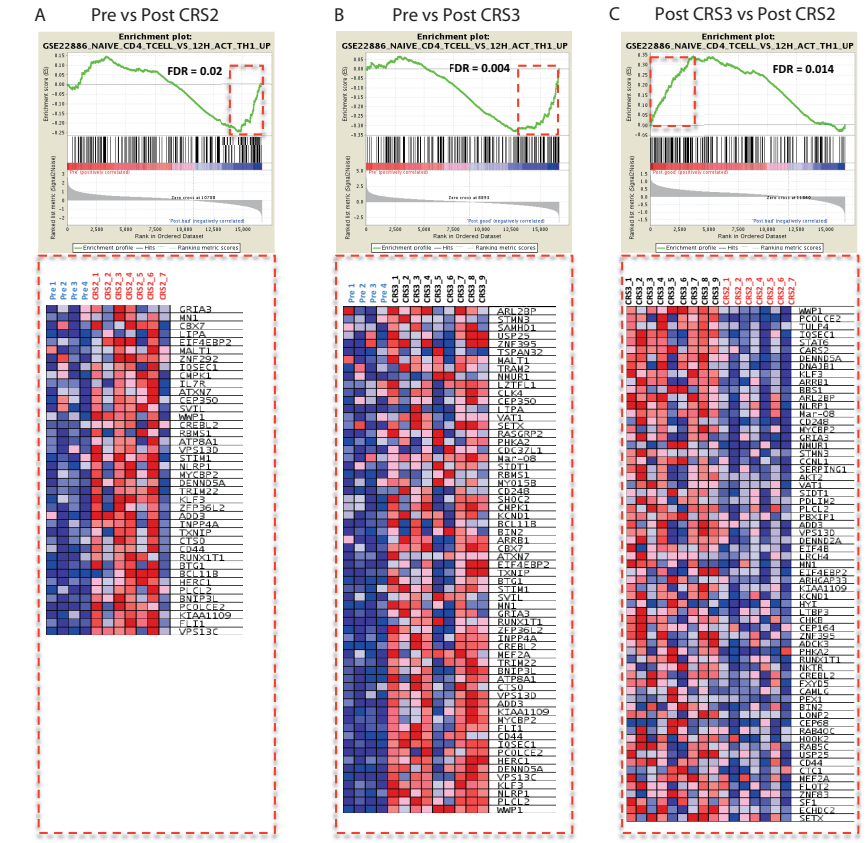
A
Pre vs Post CRS2
B
Pre vs Post CRS3
C
Post CRS3 vs Post CRS2
FDR = 0.02
FDR = 0.004
FDR = 0.014

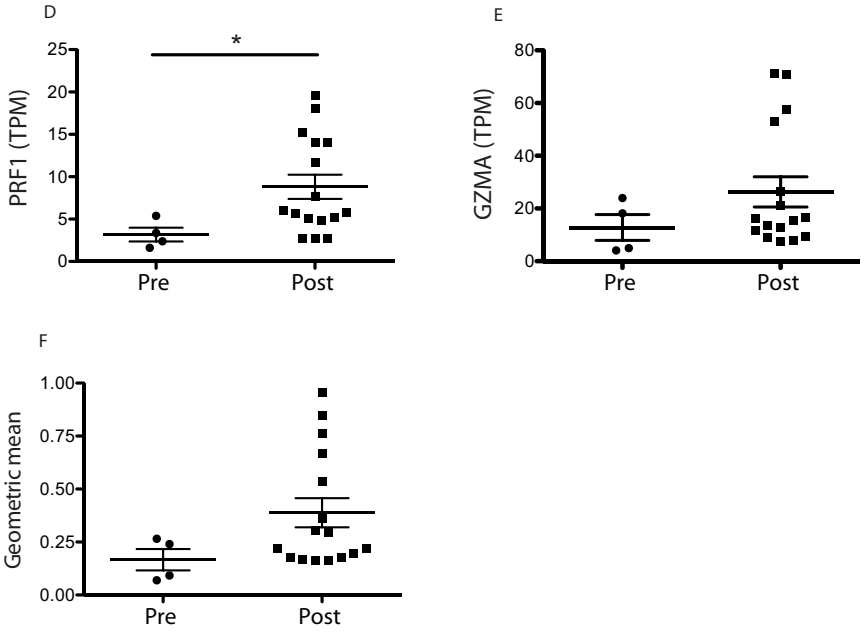
D
PRF1 (TPM)
Pre
Post
E
GZMA (TPM)
Pre
Post

F
Geometric mean
Pre
Post

Figure 5

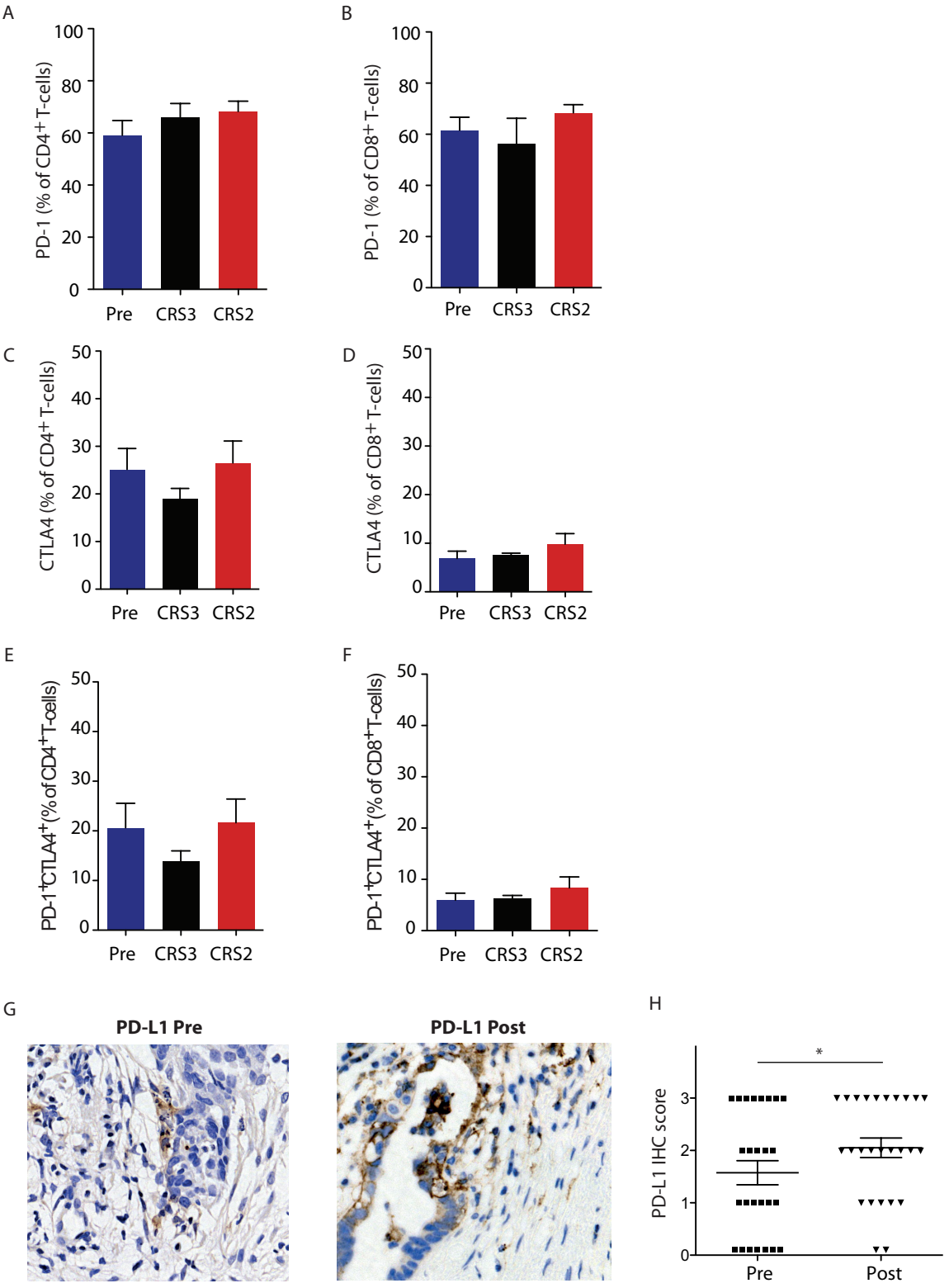
A
PD-1 (% of CD4+ T-cells)
100
80
60
40
20
0
Pre
CRS3
CRS2
B
PD-1 (% of CD8+ T-cells)
C
CTLA4 (% of CD4+ T-cells)
50
40
30
20
10
D
CTLA4 (% of CD8+ T-cells)
E
PD-1+CTLA4+(% of CD4+T-cells)
F
PD-1+CTLA4+(% of CD8+T-cells)
G
PD-L1 Pre
PD-L1 Post
H
PD-L1 IHC score
3
2
1
*
Pre
Post

Figure 6

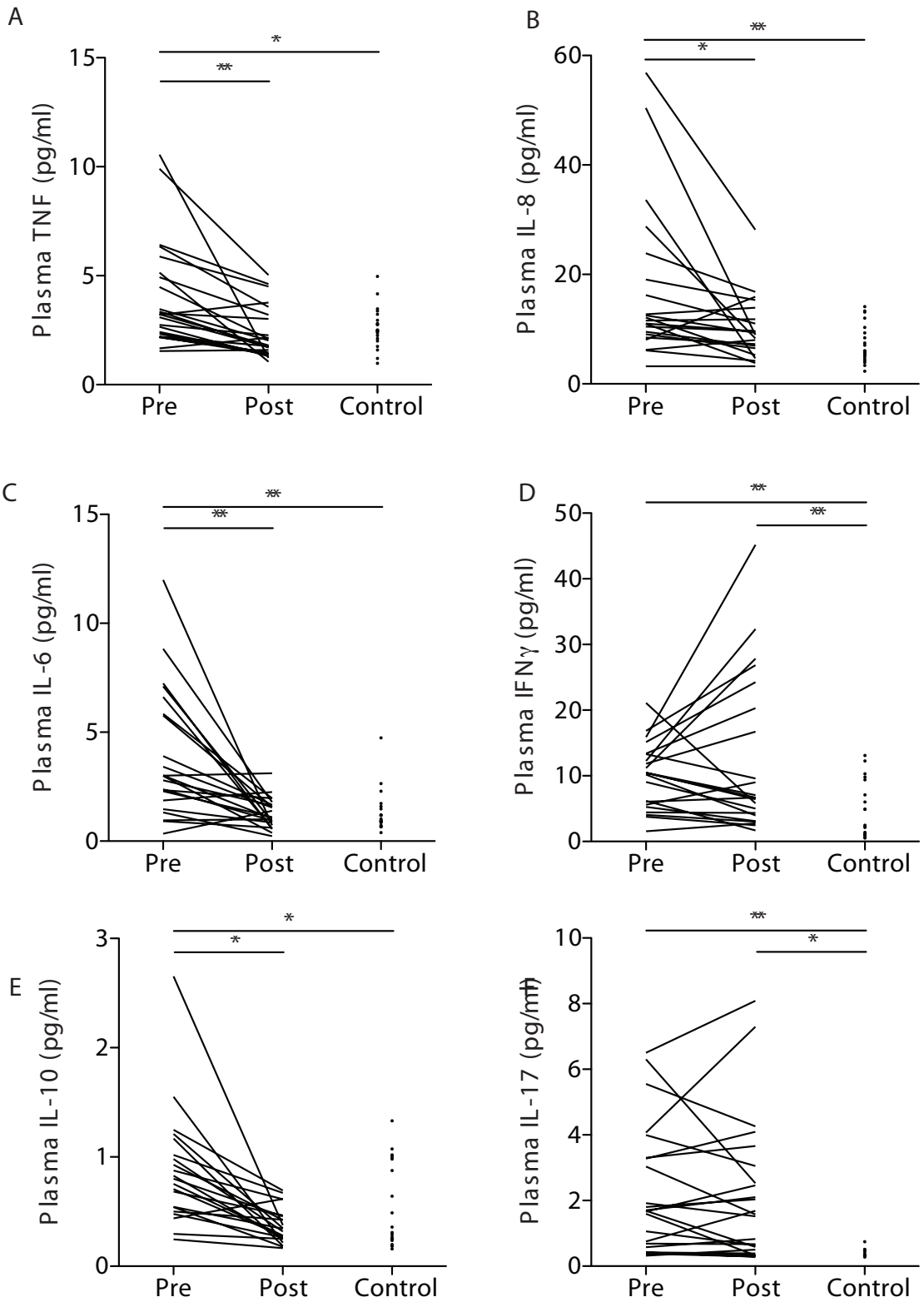
A
Plasma TNF (pg/ml)
15
10
5
0
*
**
Pre
Post
Control
B
Plasma IL-8 (pg/ml)
60
40
20
0
**
*
Pre
Post
Control
C
Plasma IL-6 (pg/ml)
15
10
5
0
**
**
Pre
Post
Control
D
Plasma IFNγ (pg/ml)
50
40
30
20
10
0
**
**
Pre
Post
Control
E
Plasma IL-10 (pg/ml)
3
2
1
0
*
*
Pre
Post
Control
Plasma IL-17 (pg/ml)
10
8
6
4
2
0
**
*
Pre
Post
Control